

# The origin of the ring current in the all-metal aromatic, $\text{Al}_4^{2-}$

Remco W. A. Havenith<sup>a</sup> and Patrick W. Fowler<sup>\*b</sup>

Received 25th May 2006, Accepted 8th June 2006

First published as an Advance Article on the web 16th June 2006

DOI: 10.1039/b607410c

**Apparent contradictions between ipsocentric, Nucleus-Independent Chemical Shift (NICS) and Gauge-Including Magnetically Induced Current (GIMIC) evaluations of ring current aromaticity in  $\text{Al}_4^{2-}$  are resolved in favour of the description of this all-metal system as  $\sigma$  aromatic on the magnetic criterion.**

## Introduction

With the detection of  $\text{MAl}_4^-$  ( $\text{M} = \text{Li}, \text{Na}, \text{Cu}$ ) cluster species by photoelectron spectroscopy,<sup>1</sup> it was recognised that small all-metal cycles could possess aromatic characteristics. The  $\text{Al}_4^{2-}$  subunit common to  $\text{LiAl}_4^-$ ,  $\text{NaAl}_4^-$  and  $\text{CuAl}_4^-$  is predicted to have a square geometry, and an electronic configuration in which 2 electrons occupy a  $\pi$  orbital. The features of planarity and equality of bond lengths, the  $2\pi$  electron count, and the delocalised nature of the  $\pi$  canonical SCF molecular orbital were taken as indicators of  $\pi$  aromaticity of this species.<sup>1</sup>

These experimental observations sparked off a number of theoretical investigations,<sup>2–9</sup> many of which focused on the question of the source of the aromaticity of this species, often invoking the magnetic criterion according to which a system is aromatic if it supports an induced ring current that flows in the same (diatropic) sense as in benzene.<sup>10–13</sup> Direct calculation using the ipsocentric method<sup>14</sup> of the current induced in  $\text{Al}_4^{2-}$  by a perpendicular external magnetic field,<sup>2</sup> confirmed the existence of a ring current with the diatropic sense, but found that this could be attributed almost entirely to circulation of  $\sigma$  electrons and not of the pair of  $\pi$  electrons that inspired the original proposal of aromaticity.

In apparent contrast with this dominance of the  $\sigma$  electrons, several studies give a greater rôle to the  $\pi$  electrons.<sup>4,8</sup> Statements to the effect that  $\text{Al}_4^{2-}$  is both  $\sigma$  and  $\pi$  aromatic can be found in several places in the literature.<sup>8,9,15,16</sup> Some are based on energy arguments, even though<sup>6</sup>  $\pi$  resonance energy in  $\text{Al}_4^{2-}$  is low, compared to that of the  $\sigma$  system here and also that of the  $\pi$  electrons of  $\text{C}_4\text{H}_4^{2+}$ . Another is based on the existence of a delocalised  $\pi$  system in this molecule, as judged from the form of the sole occupied  $\pi$  orbital, although as the SCF canonical orbitals are always delocalised, and the one orbital in this case has coefficients that are entirely determined by symmetry, the argument adds little to electron counting: there are  $4n + 2 = 2$   $\pi$  electrons in this molecule. The rest are based on magnetic properties, and as all calculations deal ultimately with approx-

imations to the same induced current density, the apparent internal contradiction is at least intriguing.

In the present paper we re-examine the theoretical evidence and suggest that, despite appearances, all available calculations are consistent with the proposal that this is a  $\sigma$  but not a  $\pi$  aromatic. The magnetically innocent rôle of the  $\pi$  electrons is fully consistent with the theory of orbital contributions that has rationalised current density calculations for a wide range of molecules.<sup>17</sup>

The two main strands of argument for significant  $\pi$  aromaticity derive from calculations of the Nucleus-Independent Chemical Shifts (NICS)<sup>13</sup> and spatial profiles obtained with the gauge-including magnetically induced current (GIMIC) method.<sup>8</sup> NICS and GIMIC evidence is discussed below, after a reprise of the original current-density results.<sup>2</sup>

## Evidence from current density maps

In the ipsocentric treatment of magnetic response,<sup>14,18,19</sup> induced current density at any point in space is calculated with that point taken as the origin of vector potential. This approach yields physically realistic patterns of current density with modest basis sets and has the specific advantage that it leads to partition of molecular magnetic properties into orbital contributions that are free of occupied–occupied mixing and are governed by symmetry selection rules.<sup>14</sup>

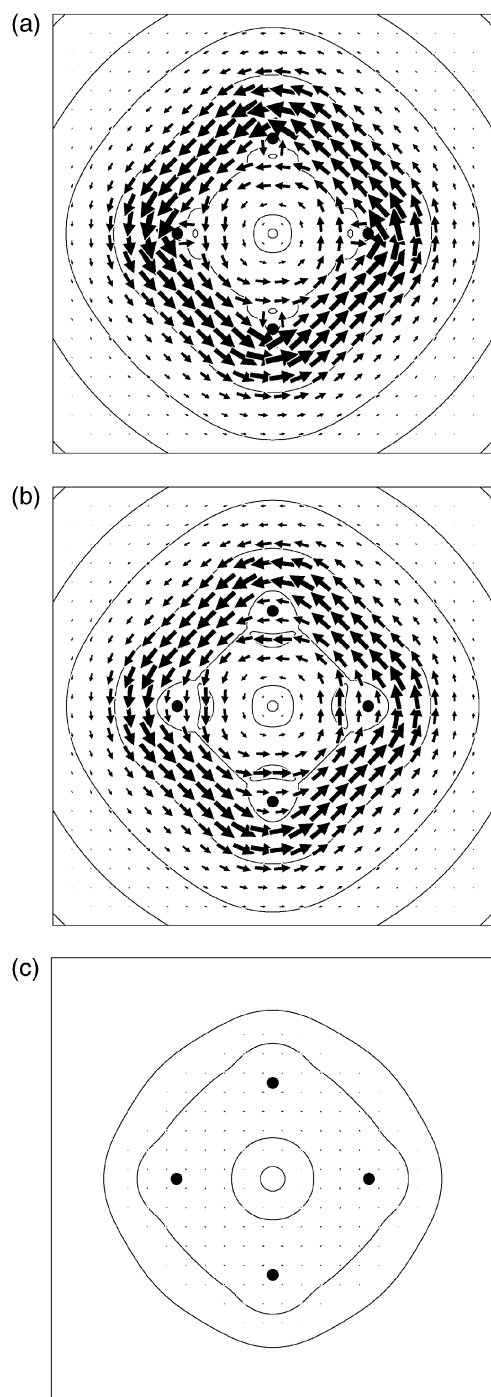
When applied to  $\text{Al}_4^{2-}$ , the ipsocentric approach predicts that application of a perpendicular magnetic field will induce a diatropic ring current (Fig. 1a), dominated by the contribution of the valence  $\sigma$  molecular orbitals (Fig. 1b), and with very little contribution from the  $2a_{2u}$   $\pi$  HOMO (Fig. 1c). For comparison, the maximum  $\pi$  current in the plotting plane is only 7% of the value obtained for benzene, whereas the total current is over 80% of the benzene standard value. In a canonical orbital picture the valence  $\sigma$  current is attributable to  $2b_{2g}$  (HOMO-2) and  $4b_{1g}$  (HOMO-3) orbitals.<sup>2</sup> As an aid to discussion of the literature results on magnetic properties, Fig. 2 and 3 give some further analysis of the response of  $\sigma$ ,  $\pi$  and  $(\sigma + \pi)$  orbitals of  $\text{Al}_4^{2-}$  to perpendicular and in-plane magnetic fields.

Fig. 2 shows height profiles of the response to a magnetic field directed parallel to the fourfold axis of  $\text{Al}_4^{2-}$ . Fig. 3 shows cross-sections of the current density induced by a magnetic field directed parallel to two edges of the  $\text{Al}_4^{2-}$  square. These illustrate two significant points, to which we will return below: that at heights above the molecular plane where the total  $(\sigma + \pi)$  response is significant, it is dominated by  $\sigma$  electrons (Fig. 2), and that the total  $(\sigma + \pi)$  response to a parallel field has a significant contribution from  $\pi$  electrons (Fig. 3).

<sup>a</sup>Theoretical Chemistry Group†, Utrecht University, Padualaan 8, 3584 CH Utrecht, The Netherlands

<sup>b</sup>Department of Chemistry, University of Sheffield, Sheffield, UK S3 7HF

†Affiliated to Organic Chemistry and Catalysis.



**Fig. 1** Current density maps for  $\text{Al}_4^{2-}$  calculated at the CTCD-DZ/6-311++G(3df)//RHF/6-311++G(3df) level.<sup>2</sup> Current density per unit inducing field is plotted in the plane  $1 a_0$  above the nuclei. The field is directed parallel to the fourfold axis, the plotting area is  $16 \times 16 a_0^2$ , the contours denote the modulus of the current density and arrows show its in-plane projection. Diamagnetic/diatropic circulation is anticlockwise. (a) Total current arising from all ( $\sigma + \pi$ ) electrons, (b) contribution from the  $\sigma$  valence orbitals, (c) contribution from the occupied  $\pi$  orbital.

#### Evidence from NICS values

Nucleus-Independent Chemical Shift<sup>13</sup> is the negative of the mean of the magnetic shielding tensor, calculated at a ring

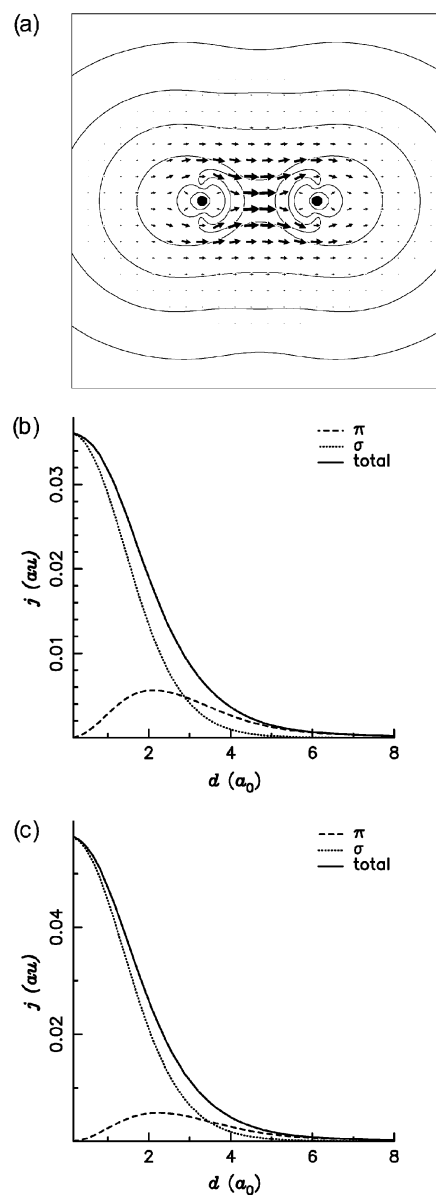


**Fig. 2** Height profile of the current density induced in  $\text{Al}_4^{2-}$  by a perpendicular magnetic field. (a) Map of the all-electron current density in a plane containing the field and the edge connecting two nearest-neighbour Al nuclei. Diamagnetic circulation is from left to right. Plotting conventions and levels of calculation are as in Fig. 1. (b) Profile of the modulus of current density in (a) against height from the molecular plane. (c) Profile in a parallel plane lying  $1 a_0$  from the edge and outside the  $\text{Al}_4$  square. In (b) and (c)  $j$  is the current density per unit inducing field and  $d$  is the height from the molecular plane, and  $\pi$ ,  $\sigma$ , and  $(\sigma + \pi)$  represent contributions of valence  $\pi$ , (summed) valence  $\sigma$ , and all orbitals, respectively.

centre (NICS(0)). A (sufficiently) negative value is taken to indicate aromaticity. Several modifications of NICS(0) exist,<sup>20,21</sup> of which one breaks up the total into contributions from canonical molecular orbitals (CMO-NICS).<sup>22</sup> CMO-NICS calculations<sup>4</sup> for  $\text{Al}_4^{2-}$  yield orbital contributions of  $-17.8$  ppm from  $\pi$ ,  $-11.1$  ppm from valence  $\sigma$  towards the total of  $-30.9$  ppm. These values are compared in Table 1 with mean central shieldings obtained by integration of the

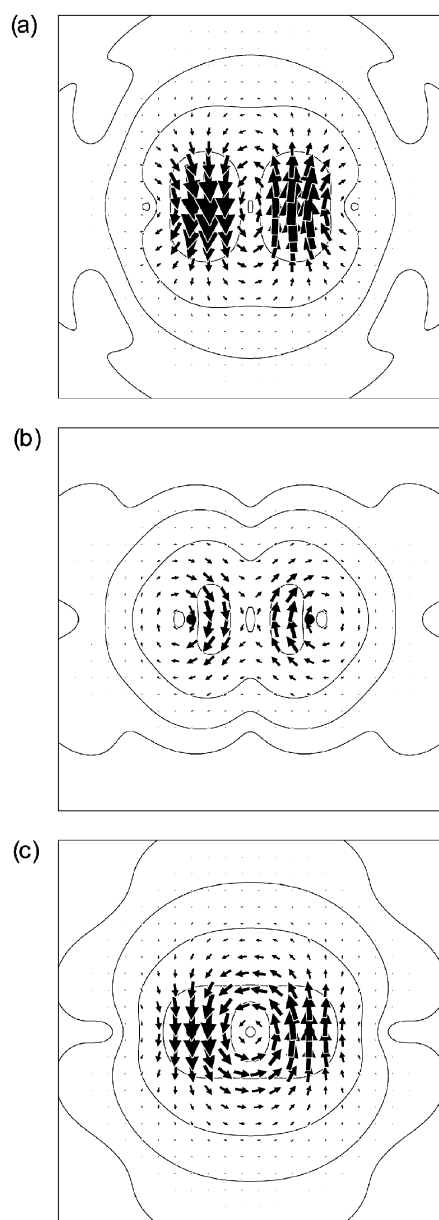


**Fig. 3** Current density maps for  $\text{Al}_4^{2-}$  calculated at the CT OCD-DZ/6-311++G(3df)/RHF/6-311++G(3df) level. Current density per unit inducing field is plotted in a plane orthogonal to that of the nuclei, parallel to an edge connecting two nearest-neighbour Al nuclei, and containing the centre of the square. The field is directed parallel to the in-plane twofold axis bisecting the edge. Other plotting conventions as in Fig. 1. (a) Total current arising from all ( $\sigma + \pi$ ) electrons, (b) contribution from the  $\sigma$  valence orbitals, (c) contribution from the occupied  $\pi$  orbital.

CT OCD-DZ (*i.e.*, ipsocentric) induced current density. Individual orbital contributions in CMO-NICS do not have the same significance as in the ipsocentric method,<sup>23</sup> and the two calculations used different basis sets and levels of theory (density functional for CMO-NICS, coupled Hartree–Fock for CT OCD-DZ), but, allowing for these differences, the trends indicated by the totals in the fourth and fifth columns of Table 1 are the same. Both methods predict NICS(0) to be dominated by the  $\pi$  contribution, which accounts for 60–70% of the total.

**Table 1** Contributions to the central NICS value in  $\text{Al}_4^{2-}$  (in ppm)

Orbital	CT OCD-DZ/6-311++G(3df) NICS(0) components			CMO-NICS <sup>a</sup>
	$xx = yy^b$	$zz^c$	Mean <sup>d</sup>	
$\pi$ ( $2a_{2u}$ )	−56.2	−6.7	−39.7	−17.8
Valence $\sigma$	6.6	−63.4	−16.8	−11.1
Core	−1.1	2.7	0.1	−2.0
Total	−50.8	−67.4	−56.3	−30.9

<sup>a</sup> NICS(0) contributions taken from ref. 4. <sup>b</sup> Negative of the in-plane component of the central shielding. <sup>c</sup> Negative of the out-of-plane component of the central shielding. <sup>d</sup> Negative of the isotropic average of the central shielding (= NICS(0)).

Taken at face value, this comparison appears to imply significant  $\sigma$  and  $\pi$  contributions to the aromaticity of  $\text{Al}_4^{2-}$ . However, aromaticity on the magnetic criterion is defined in terms of the ring current, *i.e.*, a specific response to a perpendicular magnetic field, which in turn affects one component of magnetic shielding. This component and the total NICS(0) tell different stories. Decomposition of the in- and out-of-plane components of the central shielding tensor into  $\sigma$  and  $\pi$  contributions (Table 1) reveals the source of the ‘aromatic’  $\pi$  NICS(0). The out-of-plane component of  $\pi$  shielding is small, as is consistent with the small  $\pi$  contribution to ring current (Fig. 1c). On the other hand, the in-plane component of  $\pi$  shielding is large, as is consistent with the significant current density induced in the  $\pi$ -electron distribution by a field perpendicular to the principal axis (Fig. 3c). This large component implies mobility of the  $\pi$  electron cloud, but not aromaticity—not all induced currents are *ring* currents.

Conversely, the  $\sigma$  electron distribution gives rise to a modest in-plane component of central shielding and a large out-of-plane component, a trend which is again consistent with the respective  $\sigma$  current density maps (Fig. 1b and 3b). The large  $\sigma$  contribution to NICS(0) is a direct reflection of ring current and hence of  $\sigma$  aromaticity.

This analysis shows that there is no essential disagreement between current density maps and NICS(0), as indeed there should not be, and that NICS(0) does not in fact provide evidence for  $\pi$  aromaticity of  $\text{Al}_4^{2-}$ . On the contrary, the tensor component that is directly connected to ring current shows that the aromaticity of  $\text{Al}_4^{2-}$  is  $\sigma$ - and not  $\pi$ -based. In this respect, a measure such as  $\text{NICS}_{zz}(0)$  would presumably be a better reflection of aromaticity on the magnetic criterion.<sup>20,21</sup>

### Evidence from GIMIC integrations

Calculations of current density by the GIMIC method are cited in support of  $\pi$  participation in the aromaticity of  $\text{Al}_4^{2-}$ . In ref. 8 the current density induced by a perpendicular external field is calculated for  $\text{LiAl}_4^-$  and  $\text{Li}_2\text{Al}_4$  with a CCSD wavefunction in a TZP basis of GIAO functions. This method predicts the total induced current density but does not yield individual orbital contributions. Instead  $\sigma$  and  $\pi$  contributions to the current associated with the  $\text{Al}_4^{2-}$  subunit in the two clusters are inferred indirectly as follows. First, a plane perpendicular to that of the nuclei is defined, and the total current crossing this test plane obtained by integration. Then the test plane is divided into

regions: a band between  $\pm 1.5 a_0$ , two bands  $\pm (1.5\text{--}3.5) a_0$ , and 'the rest'  $\pm (3.5\text{--}10.0) a_0$ . All current passing through the region nearest the  $\text{Al}_4$  plane is taken to be part of the  $\sigma$  contribution, all passing through the next two bands is taken to be part of the  $\pi$  contribution, and the remainder is attributed to  $\text{Li}^+$  and/or unspecified diffuse orbitals.<sup>8</sup> For example, the total current per unit magnetic field crossing the test plane is calculated to be  $32.4 \text{ nAT}^{-1}$  in  $\text{LiAl}_4^-$ , of which 16.7 is in the ' $\sigma$  region', 9.0 in the ' $\pi$  region', and  $6.6 \text{ nAT}^{-1}$  is in the outermost region.

Taken at face value, this division might appear to indicate substantial  $\sigma$  and  $\pi$  contributions to the aromaticity of  $\text{Al}_4^{2-}$ . However, as the cross-sectional maps of Fig. 2 show, a simple spatial division does not capture the distinction between  $\sigma$  and  $\pi$  current-density contributions. The contribution of the  $\sigma$  electrons is indeed maximal in the molecular plane, where the  $\pi$  contribution is zero by symmetry, but it also persists to a significant height. This is seen in the ipsocentric current profile plots of Fig. 2b and c: at its lowest, where the  $\pi$  current is maximal (7% of the benzene ring current), the crossing of  $\sigma$  and  $\pi$  curves occurs at a height of  $\sim 3 a_0$ . The profiles suggest only a minor rôle for the  $\pi$  electrons in the ring current aromaticity of  $\text{Al}_4^{2-}$ . Again, then, there is no essential contradiction between the two different magnetic-response calculations.

## Conclusion

If aromaticity is defined by the existence of ring current,  $\text{Al}_4^{2-}$  is predicted to be aromatic with an essentially  $\sigma$ -derived current. Indirect probes of the orbital origin of the current by evaluation of integrated properties, or substitution of spatial for orbital partition of current can be misleading but are not ultimately in contradiction with this conclusion.

## Acknowledgements

R. W. A. H. acknowledges financial support from the Netherlands Organisation for Scientific Research (NWO), grant 700.53.401, and P. W. F. acknowledges financial support from the Royal Society/Wolfson Research Merit Award Scheme. We

acknowledge NWO/NCF for supercomputer time on TERAS/ASTER, SARA (The Netherlands, project number SG-032).

## References

- 1 X. Li, A. E. Kuznetsov, H.-F. Zhang, A. I. Boldyrev and L.-S. Wang, *Science*, 2001, **291**, 859–861.
- 2 P. W. Fowler, R. W. A. Havenith and E. Steiner, *Chem. Phys. Lett.*, 2001, **342**, 85–90.
- 3 A. I. Boldyrev and A. E. Kuznetsov, *Inorg. Chem.*, 2002, **41**, 532–537.
- 4 Z. Chen, C. Corminboeuf, T. Heine, J. Bohmann and P. von R. Schleyer, *J. Am. Chem. Soc.*, 2003, **125**, 13930–13931.
- 5 P. W. Fowler, R. W. A. Havenith and E. Steiner, *Chem. Phys. Lett.*, 2002, **359**, 530–536.
- 6 R. W. A. Havenith and J. H. van Lenthe, *Chem. Phys. Lett.*, 2004, **385**, 198–201.
- 7 J. Jusélius, M. Straka and D. Sundholm, *J. Phys. Chem. A*, 2001, **105**, 9939–9944.
- 8 Y.-C. Lin, J. Jusélius and D. Sundholm, *J. Chem. Phys.*, 2005, **122**, 214308–214316.
- 9 C.-G. Zhan, F. Zheng and D. A. Dixon, *J. Am. Chem. Soc.*, 2002, **124**, 14795–14803.
- 10 F. London, *J. Phys. Radium*, 1937, **8**, 397–409.
- 11 L. Pauling, *J. Chem. Phys.*, 1936, **4**, 673–677.
- 12 J. Pople, *J. Chem. Phys.*, 1956, **24**, 1111.
- 13 P. von R. Schleyer, C. Maerker, A. Dransfeld, H. Jiao and N. J. R. van Eikema Hommes, *J. Am. Chem. Soc.*, 1996, **118**, 6317–6318.
- 14 E. Steiner and P. W. Fowler, *J. Phys. Chem. A*, 2001, **105**, 9553–9562.
- 15 A. I. Boldyrev and L.-S. Wang, *Chem. Rev.*, 2005, **105**, 3716–3757.
- 16 Z. Chen, C. S. Wannere, C. Corminboeuf, R. Puchta and P. von R. Schleyer, *Chem. Rev.*, 2005, **105**, 3842–3888.
- 17 P. W. Fowler, E. Steiner, R. W. A. Havenith and L. W. Jenneskens, *Magn. Reson. Chem.*, 2004, **42**, S68–S78.
- 18 T. Keith and R. F. W. Bader, *Chem. Phys. Lett.*, 1993, **210**, 223–231.
- 19 P. Lazzeretti, M. Malagoli and R. Zanasi, *Chem. Phys. Lett.*, 1994, **220**, 299–304.
- 20 C. Corminboeuf, T. Heine, G. Seifert, P. von R. Schleyer and J. Weber, *Phys. Chem. Chem. Phys.*, 2004, **6**, 273–276.
- 21 H. Fallah-Bagher-Shaldael, C. S. Wannere, C. Corminboeuf, R. Puchta and P. von R. Schleyer, *Org. Lett.*, 2006, **8**, 863–866.
- 22 T. Heine, P. von R. Schleyer, C. Corminboeuf, G. Seifert, R. Reviakine and J. Weber, *J. Phys. Chem. A*, 2003, **107**, 6470–6475.
- 23 E. Steiner and P. W. Fowler, *Phys. Chem. Chem. Phys.*, 2004, **6**, 261–272.